IJMCM
International Journal of Molecular and Cellular Medicine
p-ISSN: 2251-9637 o-ISSN: 2251-9645
Babol University of Medical Sciences
Cellular and Molecular Biology Research Center

Combination Therapy in Cancer: Doxorubicin in Combination with an N-terminal Peptide of Endostatin Suppresses Angiogenesis and Stimulates Apoptosis in the Breast Cancer

Narges Sarabi[1], Reyhane Chamani[2]*, Elham Assareh[1], Omid Saberi[1], S. Mohsen Asghari[3]

1. Department of Biology, Faculty of Sciences, University of Guilan, Rasht, Iran.
2. Department of Biology, Yazd University, Yazd, Iran.
3. Institute of Biochemistry and Biophysics, University of Tehran, Tehran, Iran.

Article type: **Original Article**

Received: 2023.04.23
Revised: 2023.10.12
Accepted: 2023.11.12

ABSTRACT

The combination of chemotherapy drugs with angiogenesis inhibitors improves response and survival and reduces the cytotoxic side effects and drug resistance in patients compared to chemotherapy alone. Here, we investigated the efficacy of the concomitant administration of doxorubicin and a peptide derived from the N-terminal domain of Endostatin (called ES-SS) in the 4T1 mammary carcinoma tumor model. Tumor-bearing mice were divided into the control and three treatment groups, including ES-SS, doxorubicin, and the combination. Injections were performed daily for two weeks and tumor volumes were measured during the treatment. Immunohistochemical analysis of Ki-67, CD31, CD34, Bcl-2, p53 expression, and TUNEL assay were performed on tumor tissues at the end of treatment. Besides, molecular dynamics and docking simulations were performed. It was demonstrated that tumor growth was inhibited in mice treated with peptide plus doxorubicin more significantly than in each treatment alone ($P<0.05$). No weight loss or adverse effects were observed. Moreover, combination therapy was more effective in tumor angiogenesis suppression and apoptosis stimulation ($P<0.05$). Docking simulations by ClusPro server demonstrated that ES-SS binds to integrin α5β1, Transglutaminase 2, and Matrix metalloproteinase 2 with more negative binding energy and hydrogen bonds compared to the native peptide. Generally, we proposed that ES-SS can augment the therapeutic efficacy of doxorubicin through angiogenesis prevention and apoptosis induction in breast tumor. Owing to the advantages of peptides to recombinant proteins or monoclonal antibodies, further preclinical and clinical evaluations of this combination strategy are worth taking into consideration.

Keywords: Angiogenesis inhibitor, apoptosis, breast cancer, doxorubicin, endostatin

Cite this article: Sarabi N, *et al*. Combination Therapy in Cancer: Doxorubicin in Combination with an N-terminal Peptide of Endostatin Suppresses Angiogenesis and Stimulates Apoptosis in the Breast Cancer. *International Journal of Molecular and Cellular Medicine. 2023; 12(2):120-134.* **DOI:** 10.22088/IJMCM.BUMS.12.2.120

***Corresponding:** Reyhane Chamani
Address: Department of Biology, Yazd University, University Blvd, Safayieh, Yazd, Iran.
E-mail: chamani@yazd.ac.ir

Introduction

Over the past two decades, there was much interest in discovering and developing angiogenesis inhibitors for cancer therapy. Numerous candidates have entered a clinical trial or achieved approval for clinical use, ranging from monoclonal antibodies and endogenous proteins to small molecules. In this regard, many studies have been conducted on Endostatin, an endogenous angiogenesis inhibitor. Findings confirmed the safety and efficacy of Endostatin in treating different types of cancers in animal models and clinical trials (1,2). Currently, endostatin, under the trade name of Endostar, has been evaluated in clinical trials in China, mainly in combination with chemotherapy for treating various types of cancers like non-small cell lung and breast cancers (3,4). Due to the complexity of recombinant protein production and unaffordable cost, researchers are developing synthetic peptides as an alternative to full-length protein. Javaherian *et al*. demonstrated that a 27 amino acid peptide derived from the N-terminal of endostatin can suppress angiogenesis and growth of tumors in mice comparable to full-length protein (5). Besides, Chamani *et al*. developed a peptide so called ES-SS, comprising some modifications to the abovementioned peptide, and demonstrated that ES-SS was more potent than wild-type peptide in preventing angiogenesis and growth of mammary adenocarcinoma in mice (6).

Despite the widespread research for discovering new methods for curing patients, cytotoxic chemotherapy is one of the main treatment approaches for cancer. However, this method suffers from some essential disadvantages like toxic side effects, lack of tumor cell selectivity, and the development of drug resistance (7). Therefore, to cope with these problems, the combination of chemotherapy with other treatments was proposed (8) and investigated extensively. Various surveys confirmed that combination therapy leads to a superior response and enhanced survival compared to monotherapy (9). For example, studies showed that combination of TAS-102 (trifluridine/ tipiracil) with antiangiogenic agent Bevacizumab significantly increases the median overall survival and median progression-free survival in patients with metastatic colorectal cancer (10). Results of a cohort study on patients with advanced non-small cell lung cancer showed that patients received Programmed cell Death protein 1 (PD-1)/Programmed cell Death-Ligand protein 1 (PD-L1) inhibitors plus anti-angiogenic agents plus chemotherapy had a longer progression free survival and overall survival as well as downtrend in the risk of disease progression and death (11). In this strategy, because of synergistic or additive effects of two (or more) treatments, the application of lower doses of chemotherapy in fewer cycles reduces the incidence of drug resistance (12) and cytotoxic effects but augment efficacy is extremely important in a successful treatment regimen (13). The tumor microenvironment has an unusual vasculature characterized by amplified vessel permeability, tortuosity, reduced pericyte coverage, abnormal basement membranes, and high interstitial fluid pressure within tumors. These features lead to ineffective delivery of oxygen and therapeutic drugs into tumors (14). Angiogenesis inhibitors possibly will normalize the tumor microenvironment, leads to improved transport of chemotherapy drugs into the tumor tissue, providing a “window of opportunity” for the delivery of drugs, as Jain et al. stated in the theory of “vascular normalization” (15). On the other hand, clinical trials have revealed that antiangiogenic monotherapy with drugs such as Bevacizumab and Sunitinib could induce drug resistance in patients due to the activation of alternative pathways for tumor vascularization and growth. Combination of

[DOI: 10.22088/IJMCM.BUMS.12.2.120]

angiogenesis inhibitor with chemotherapy has increased the success of the antiangiogenic treatments through different mechanisms (16).

Doxorubicin is used widely for the treatment of breast cancer; however, single-agent chemotherapy may result in developing drug resistance as well as cytotoxic side effects such as cardiotoxicity, which is the main adverse effect of doxorubicin (17). To minimize these challenges, concurrent use of chemotherapy with biological drugs was investigated largely. In this regard, the combination of chemotherapy with angiogenesis inhibitors may be beneficial via different mechanisms, includes morphologic normalization of tumor vasculature (15), preventing regrowth of tumor cells between courses of chemotherapy (18), and disruption of tumor vasculature in low dose (19). In addition, relieving the tumor's immunosuppressive environment recovers delivery of immune cells into the tumor, results in the motivation of the host immune system against the tumor (20). Recently, we have shown that ES-SS can modulate the immunosuppressive microenvironment and activate cellular and humoral immunity in tumors by TNF-α, IL-10, IFN-γ, IL-4, and IL-17 production elevation in mice (21).

Despite the benefits of anti-angiogenic therapy, this strategy limits for some reasons like heterogeneity of endothelial cells, induction of hypoxia in tumors leading to secretion of other angiogenic factors, and dramatic inhibition of tumor vascularization leading to reduced delivery of chemotherapeutic agents. Combination with other treatments like chemotherapy, optimal dosing and scheduling may improve patients outcomes (22). The present study aimed to investigate the anti-tumor, anti-angiogenic and anti-apoptotic effects of ES-SS in combination with doxorubicin in a mouse mammary carcinoma tumor model. Furthermore, we performed molecular dynamics and docking simulations to evaluate the interaction of the peptide to the receptors involved in its anti-angiogenic activity compared to the native one.

Materials and methods

Peptide and reagents

Shine Gene Biotechnologies, Inc. (Shanghai, China) synthesized the peptide with a purity of ~95% assessed by analytical high-performance liquid chromatography, analyzed by matrix-assisted laser desorption/ionization time-of-flight mass spectrometry (MALDI-TOF), and confirmed by electrospray ionization mass spectrometry (ESI-MS) analysis. Doxorubicin purchased from *BORYUNG* Pharmaceutical Co., Ltd. (Seoul, Korea South). Anti-CD31 (Ab32457), anti-CD34 (Ab81289), anti-Ki67 (Ab15580), anti-p53 (Ab131442), and anti-Bcl-2 (Ab59348) were from Abcam, Cambridge, UK, and TUNEL assays were performed using an *in situ* Cell Death Detection Kit POD (Roche Diagnostic GmbH, Germany).

Molecular dynamics simulations

The firs 27 amino acid from N-terminal of human endostatin was extracted from the PDB of human endostatin (PDB ID: 1BNL) and was considered as a native fragment (ES-Zn). Structural models for ES-SS were constructed by MODELLER 9 program based on the native peptide ES-Zn. A disulfide bond was inserted into the structure by Hyperchem program (Hypercube, Inc.). Then, explicit water solvation was used to refine structures. Molecular dynamics simulations were performed using GROMACS 4.5.5 package (23). Simple point charge (SPC) water and a cubic box with 1 nm of solvent on all sides were used to solve peptides. The simulation cells were neutralized by replacement of water molecules by Na^+ and Cl^- ions. The

[DOI: 10.22088/IJMCM.BUMS.12.2.120]

pressure and the temperature were 1 bar and 310 K, respectively, by Berendsen algorithm. The energy minimization was performed by steepest descent energy minimization. The systems were simulated for 100 picoseconds by canonical ensemble where the amount of substance (N), volume (V) and temperature (T) was constant. The equilibration step was finalized under 1000 picoseconds where the amount of substance (N), pressure (P) and temperature (T) was constant. Each system was simulated at 300 K for 100 ns. The analyses were carried out at 0.5 ps time intervals from the simulations. Finally, the amount of Root Mean Square Deviation (RMSD), Root Mean Square Fluctuation RMSF, and Dictionary of Secondary Structure of Proteins (DSSP) were obtained (24).

Molecular docking simulations

Interaction of peptides with integrin α5β1 (PDB ID: 7NXD), Transglutaminase 2 (PDB ID: 2Q3Z), and Matrix metalloproteinase 2 (PDB ID: 1CK7) was predicted by ClusPro docking server version 2.0. ClusPro is a fully automated web server for the prediction of protein-protein interactions. The program recruits PIPER, a Fast Fourier Transform (FFT) based rigid docking program, to generate 1000 low energy docked conformations using pairwise interaction potentials. The program then clusters these conformations and ranks the clusters by ClusPro algorithm (25). Ligand-receptor interactions including hydrogen bonds were analyzed by PyMOL software. To display hydrogen bonds in this software, user should find polar contacts to other atoms in object. It displays all possible hydrogen bonds with bond distance between donor and acceptor. Salt bridges were computed by What if web server (https://swift.cmbi.umcn.nl/servers/html/shosbr.html). A salt bridge is composed of a negative atom and a positive atom with an interatomic distance less than 7.0 Angstrom. PDB of ligand-receptor complex was uploaded in the server. The distance of formed salt bridges is displayed in the result page in the server.

4T1 Cell culture

The mouse mammary carcinoma cells (4T1) were purchased from the Iranian Biological Resource Center (Tehran, Iran). The cells were cultured in DMEM medium supplemented with 10% heat-inactivated FBS, 100 U/mL penicillin, and 100 µg/mL streptomycin and incubated at 37°C in a humidified atmosphere of 5% CO2. Cells at 80-90% confluence (passage 3) were used for injection.

Generation of 4T1 mammary tumor in mice and treatment schedule

Thirty-two female BALB/c mice (5-7 weeks) were purchased from Pasteur Institute of Iran (Tehran, Iran) and used for experimental purposes with the approval of the Institutional Animal Care and Use Committee (IACUC) of Tehran University of Medical Sciences. All animals were maintained under a 12-hour dark and light cycle, with free access to food and water. 4T1 cell suspensions (7×10^5 cells) in 100 Ml DMEM were injected subcutaneously into the right flank of mice. The tumor length (a) and width (b) were measured every other day, and the tumor volume (V) was calculated by the following formula: V (mm3) = $(a \times b^2) \times 0.52$. When tumors reached around 100 mm^3 in about 10 days, mice were randomly divided into three treatment groups (n=8): ES-SS, doxorubicin, and ES-SS + doxorubicin, and a control group (n=8). In ES-SS and ES-SS + doxorubicin groups, mice received an i.p. injection of 2.5 mg/kg/day of peptide every day. In doxorubicin and ES-SS + doxorubicin groups, mice received an i.p. injection of 6 mg/kg/day of Doxorubicin two times a week. Control group was administered i.p. injection of 100 µl of phosphate buffer saline (PBS). All treatments were administered for two weeks and included 8 mice per group. Furthermore,

[DOI: 10.22088/IJMCM.BUMS.12.2.120]

animal body weights were measured and mice were observed regularly for any unusual signs and adverse effects. At the end of the study, mice were sacrificed under ketamine (100 mg/kg, i.p.) and xylazine (10 mg/kg, i.p.) anesthesia and tumor tissues were isolated and fixed in formalin.

Immunohistochemical staining of Ki-67, CD31, CD34, Bcl-2 and p53 markers

Immunohistochemistry studies were performed using specific antibodies according to the manufacturer's instructions. Briefly, 3- to 5-µm tissue sections were taken from the formalin-fixed paraffin blocks and were deparaffinized with xylene and rehydrated by a series of ethanol solutions with descending grades. The slides were placed in Tris-buffered saline- Ethylenediaminetetraacetic acid (TBS-EDTA) buffer and heated for 15 min at 90 °C. Incubation in a 0.3% H_2O_2 buffer for 15 min was performed to block endogenous peroxidase activity. Ki-67, CD31, CD34, Bcl-2 and p53 primary antibodies were added. Then, the biotinylated secondary antibodies, avidin-biotin complex with horseradish peroxidase and finally the chromogenic 3, 3'-diaminobenzidine substrate (Sigma Chemical) were added. Images of stained sections were acquired by microscopy (Olympus BX-51, Japan). Ten randomly chosen fields under scale bars 100 and 20 µm were analyzed for determining positive cells with Image J software. Results of CD31 and CD34 staining, two angiogenesis markers, were expressed as the average of microvessels per field and results of Ki-67, Bcl-2, and p53 staining were stated as percentages of positive cells per field.

Detection of apoptosis by TUNEL assay

To detect apoptosis in tumor tissues, the Terminal deoxynucleotidyl transferase-mediated dUTP nick-end labeling (TUNEL) assay was carried out according to the protocols of the manufacturer (Roche Diagnostic GmbH, Germany). Briefly, Paraffin-embedded tumor sections were deparaffinized in water and placed in 3% H_2O_2 for 10 min at room temperature. Then, slices were treated with proteinase K solution for permeation. The slides were immersed in terminal deoxynucleotidyl transferase (TdT) labeling buffer. Then samples were covered with anti-bromodeoxyuridine (anti-BrdU) and incubated with streptavidin horseradish peroxidase (HRP) solution. Diaminobenzidine (DAB) was used as the chromogen and tissue sections were counterstained with methyl green. The slides were viewed in a blinded fashion. TUNEL-positive cells (brown-stained) were counted as a percentage of the total cells in ten randomly chosen high-power fields under scale bars 100 and 20 µm, with quantification using Image J.

Statistical analyses

The Prism software (version 6.00 for Windows, GraphPad Software, La Jolla, California, USA; www.graphpad.com) was used for data analysis, the generation of graphs, and for statistical analysis. Analysis of different data between groups was performed using one-way ANOVA followed by Turkey's test. Values were expressed as the mean ± SEM. The probability values less than 5% ($P<0.05$) were considered significant and it was indicated by asterisks in the figures.

Results

Structural and binding analysis by MD and docking simulations

Since the anti-angiogenic and anti-tumor activities of endostatin mediated by its interaction with various enzymes and receptors, we decided to compare the interaction of peptides ES-Zn and ES-SS with integrin α5β1, Transglutaminase 2, and Matrix metalloproteinase 2 using molecular docking simulation. So, the

[DOI: 10.22088/IJMCM.BUMS.12.2.120]

structure of the peptides simulated by GROMACS program. Then, the resulting PDB was used for docking simulation.

MD simulations were carried out for 100 ns. The structures were stable during the simulations as demonstrated by the Root Mean Square Deviation (RMSD) of the Cα backbone in Figure 1A. Root Mean Square Fluctuation (RMSF) indicates the measure of flexibility for each residue. Calculation of RMSF demonstrated that in ES-SS overall fluctuation for most residues is lower than the native peptide (Figure 1B). Dictionary of Secondary Structure of Proteins (DSSP) designates the secondary structures during simulation. As shown in Figure 1C, the number of secondary structure, including β-sheet, β-turn, bend, and helices in ES-SS are more than wild-type, which may explain the lower fluctuation of the residues.

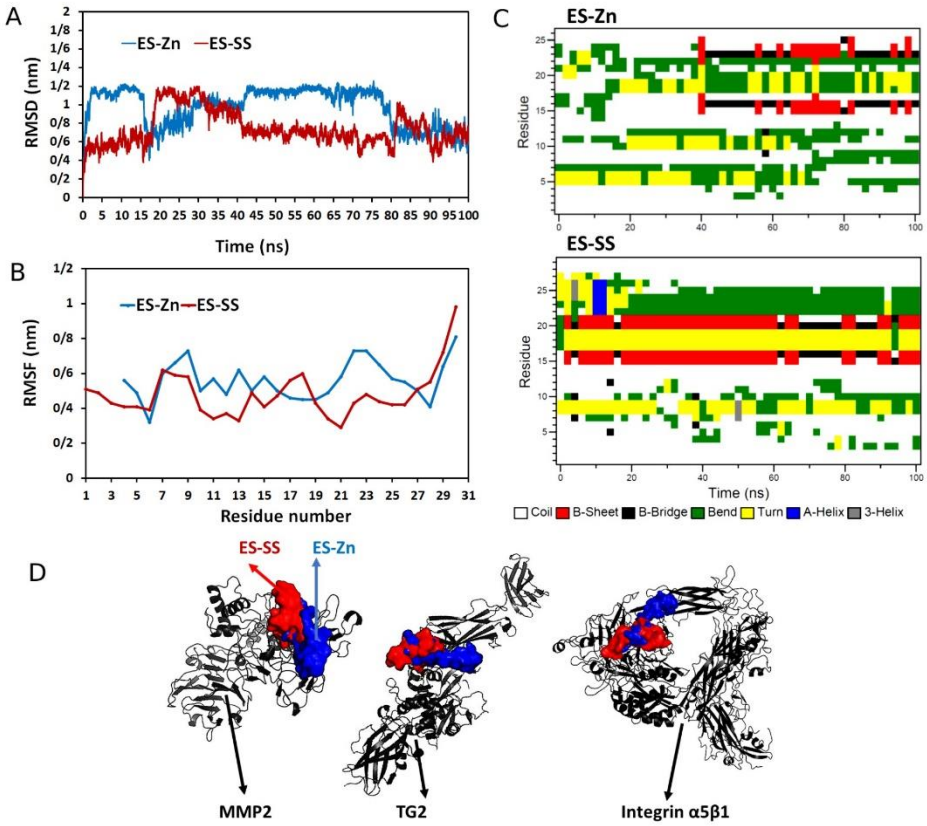

Fig.1. Molecular dynamics and docking simulations. MD simulations were performed using GROMACS 4.5.5 package for 100 nanoseconds. A) RMSD of the Cα backbone of the native (ES-Zn, blue line) and engineered peptides (ES-SS, red line) derived from endostatin. B) RMSF of residues of ES-Zn (blue line) and ES-SS (red line). C) Secondary structures of the peptides during simulations (100 ns). D) Docking simulations of the peptides were performed using ClusPro 2. MMP-2, TG-2, and integrin α5β1 were shown as black ribbons. ES-Zn and ES-SS were demonstrated as blue and red spheres, respectively. Complexes were depicted using PyMOL software.

ClusPro v. 2.0 was used for the interaction prediction of peptides with integrin α5β1, Transglutaminase 2, and Matrix metalloproteinase 2. The best complex, consisting of the lowest energy and maximum cluster member, was analyzed by PyMOL. As demonstrated in figure 1D, peptides bind similarly to the integrin α5β1, Transglutaminase 2, and Matrix metalloproteinase 2, but the binding energy of ES-SS was lower than ES-Zn (Table 1).

[DOI: 10.22088/IJMCM.BUMS.12.2.120]

Table 1. Binding energy (kcal/mol) of complexes resulted from docking simulations

Receptor	Ligand	Cluster member	Lowest energy (Kcal/mol)
Matrix metalloproteinase 2	ES-Zn	68	-894.7
	ES-SS	102	-1147.6
Transglutaminase 2	ES-Zn	216	-990.6
	ES-SS	164	-1141.9
Integrin α5β1	ES-Zn	140	-1191.8
	ES-SS	141	-1379.6

Hydrogen bonds formed between the ligand and the receptor usually contribute to the stability of the complexes; more number hydrogen bonds create more stable complexes. Assessment of hydrogen bonds by PyMOL software demonstrated that all docked complexes with ES-SS stabilized by more hydrogen bonds than ES-Zn complexes (Table 2).

Table 2. Hydrogen bonds and salt bridge distances between peptides and receptors

Receptor	H-bonded residues in receptor	Peptide	H-bonded residues in peptide	Salt bridge distance (nm)
Transglutaminase 2	Q348, S385, K384, T457, E503,	ES-Zn	S2, H3, Q7, S20, R27	2.93
Transglutaminase 2	Q329, K364, S365, N460, N531, R569	ES-SS	S5, D8, H14, C19, S23, R30	2.67
Matrix metalloproteinase 2	R175, D210, S304, T307, E345	ES-Zn	H1, H3, D5, R27	2.85
Matrix metalloproteinase 2	R175, D210, H276, Q289, S304, E345	ES-SS	R7, Q10, S20, S23, R27	2.49
Integrin α5β1	K41, E91, S97, R184, E284	ES-Zn	H1, R4, D5, Q7, R27	2.78
Integrin α5β1	K4, T171, S291, H299, Q380, H410	ES-SS	S5, R7, D8, Q10, S23, R30	2.57

The salt bridge between positive and negative charge amino acids is significant for the stabilization of the protein's structure and ligand-receptor complex (26). Salt bridges between peptides and receptors were calculated by the What if web server. They formed with stable distances in all complexes; however, the distances were shorter in ES-SS complexes than those in ES-Zn. The salt bridge with the shortest distance stabilizes the complex the most.

Mammary tumor growth inhibition in mice

As indicated in Figure 2, treatment of mice with 2.5 mg/kg/day ES-SS peptide or 6 mg/kg/day doxorubicin inhibited tumor growth by 21% and 37%, respectively. Combination of ES-SS with doxorubicin resulted in an inhibitory effect of 53% on tumor growth compared to control ($P<0.001$). In addition, body weights increased weekly in all groups. Mice were monitored regularly for unusual signs and adverse effects like lethargy, hunched posture, and poor grooming (rough hair coat). No adverse signs were observed during the treatment. Mice in all groups survived until the end of the study.

[DOI: 10.22088/IJMCM.BUMS.12.2.120]

Inhibition of proliferation in tumors

Ki-67 is a significant cellular marker to determine cell proliferation in breast tumors. Immunostaining of tumor sections showed that the percentage of Ki-67 positive cells decreased significantly in ES-SS (P=0.011), doxorubicin (P=0.011), and combination therapy (P=0.0002) groups compared to control (Figures 3A and 3B) indicating the inhibitory effect of these treatments on the proliferation and growth of tumor cells. In addition, as demonstrated in figure 3B, the percentage of Ki-67 positive cells decreased in combination therapy much more than monotherapy groups (P=0.011 and P= 0.0069).

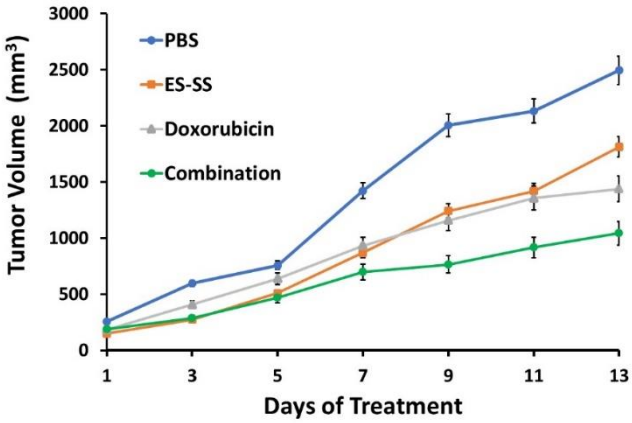

Fig.2. Inhibition of 4T1 mammary tumor growth**.** Mice (n=8/groups) received i.p. injection of 2.5 mg/kg/day of peptide (ES-SS) every day or 6 mg/kg/day of doxorubicin two times a week. In the combination group, mice received 2.5 mg/kg/day of peptide every day and 6 mg/kg/day of doxorubicin two times a week, concurrently. All treatments were administered for two weeks. Tumor volume (V) was calculated by following formula: $V\ (mm^3) = (a \times b^2) \times 0.52$. Each point represents the mean value of 8 treatments in each group. The error bars are equivalent to SEM ($P < 0.001$).

Prevention of angiogenesis in tumor tissues

We exploit two angiogenesis markers, CD31 and CD34, to evaluate tumor vascularization (Figure 3A). Positive immunostained cells were counted, and results were expressed as the average microvessel per field. Our results demonstrated that ES-SS, doxorubicin, and combination therapy groups significantly inhibited angiogenesis in breast tumor tissue compared to control (P<0.0001) (Figures 3C and 3D). Furthermore, combined treatment of mice with ES-SS and doxorubicin significantly reduced the expression of CD31 and CD34 more potent than each treatment alone (P< 0.001) (Figures 3C and 3D

Examination of apoptosis induction in tumor tissues

The expression of Bcl-2, an anti-apoptotic protein, and p53 tumor suppressor was evaluated by immunohistochemistry to determine the induction of apoptosis in tumor tissues (Figure 4A). Results showed that the percentage of Bcl-2 positive cells reduced significantly in sections treated with ES-SS (P=0.04), doxorubicin (P=0.001), and combination therapy (P<0.0001) compared to control (Figure 4B). Moreover, combining ES-SS and doxorubicin declined the expression of Bcl-2 in tumors more than in each treatment alone (P= 0.04) (Figure 4B). As demonstrated in figure 4C, ES-SS (P=0.03), doxorubicin (P=0.0034), and combination therapy (P<0.0001) boosted the percentage of p53 positive cells in sections compared to the control and concurrent use of these treatments was significantly more effective than monotherapy (P<0.0001).

[DOI: 10.22088/IJMCM.BUMS.12.2.120]

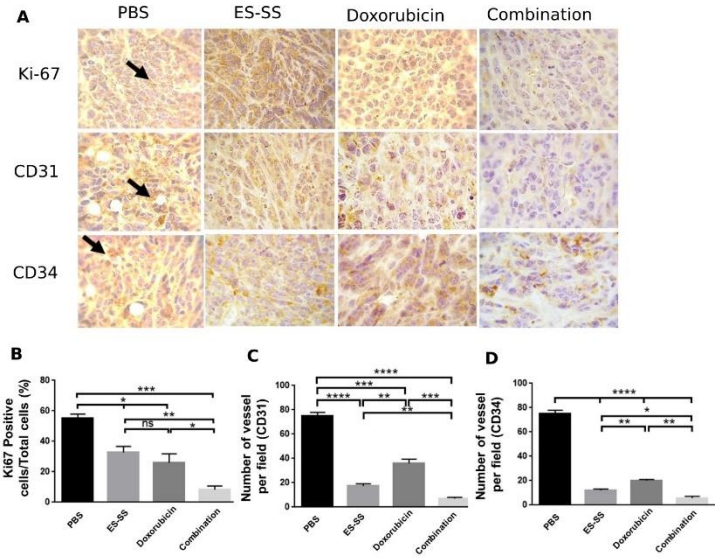

Fig.3. Immunohistochemical evaluation of angiogenesis and proliferation in tumors. A) Photographs of immunostained sections using related antibodies (400× magnification) (Peptide: ES-SS, Combination: ES-SS + Doxorubicin). B) Percentage of Ki-67 positive cells per total cells in field in tumor sections. Error bars are equivalent to SEM (* P= 0.011, ** P= 0.0069, *** P= 0.0002). C) Average of CD31 positive blood vessel count per field in tumor sections. Each column represents the mean value of eight treatments in each group and error bars are equivalent to SEM (** P=0.008, *** P=0.001, **** P < 0.0001). D) Average of CD34 positive blood vessel count per field in tumor sections. Error bars are equivalent to SEM (* P= 0.027, ** P= 0.001, **** P < 0.0001).

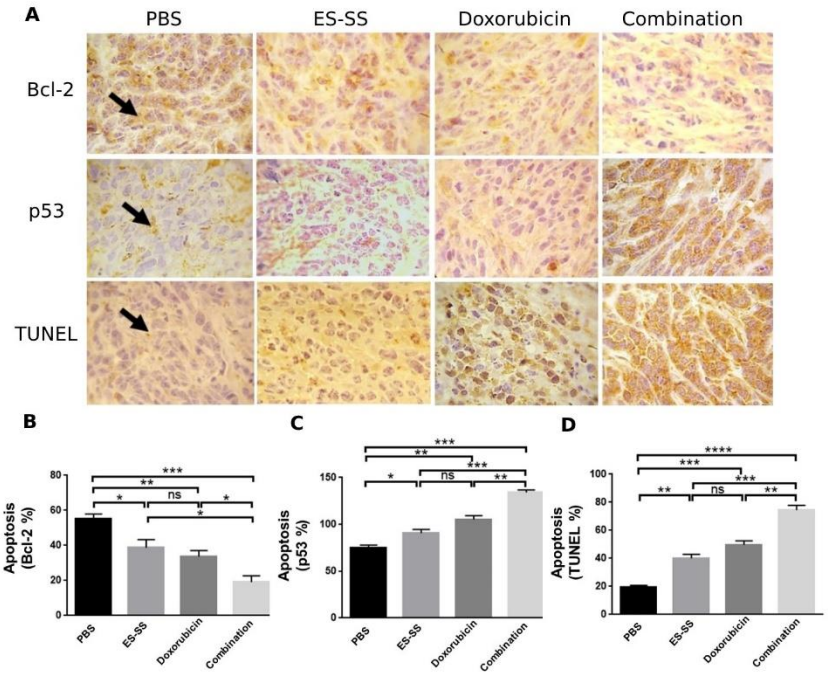

Fig.4. Induction of apoptosis in tumors. A) Photographs of tumor sections stained by antibodies using immunohistochemistry (400× magnification) (Peptide: ES-SS, Combination: ES-SS+Doxorubicin). B) Percentage of Bcl-2 positive cells per total cells in immunostained tumor sections. Error bars are equivalent to SEM (* P= 0.04, ** P= 0.001, *** P < 0.0001). C) Percentage of p53 positive cells in immunostained tumor sections. Error bars are equivalent to SEM (* P= 0.03, ** P= 0.0034, *** P < 0.0001). D) Percentage of TUNEL positive cells in immunostained tumor sections. Error bars are equivalent to SEM (** P= 0.003, *** P= 0.0007, **** P < 0.0001).

[DOI: 10.22088/IJMCM.BUMS.12.2.120]

Detection of apoptosis in tumor tissue by TUNEL staining

To further evaluate the induction of apoptosis in tumor tissues, we employed TUNEL staining, a method for detecting DNA fragmentation by labeling the 3′-hydroxyl termini in the double-strand DNA breaks generated during apoptosis and counting the number of TUNEL-positive cells (Figure 4A). As demonstrated in figure 4D, the percentage of apoptotic cells increased significantly in tumors treated with peptide ($P=0.003$), doxorubicin ($P=0.0007$), or combination therapy ($P<0.0001$) compared to the control, and combining treatment with ES-SS and doxorubicin had a superior effect on stimulation of apoptosis in comparison to monotherapy ($P<0.0001$).

Discussion

In the current study, we demonstrated that the engineered N-terminal fragment of endostatin (ES-SS) interacts with the integrin α5β1, transglutaminase 2, and matrix metalloproteinase 2 with lower binding energy and more hydrogen bonds compared to the native peptide. Moreover, concurrent administration of ES-SS with doxorubicin suppresses mammary carcinoma growth more potent than each treatment individually. ES-SS or doxorubicin could inhibit vascularization and proliferation and trigger apoptosis in tumor tissues. However, combination of ES-SS and doxorubicin was more effective, possibly due to synergistic effects between the agents. It is the first study demonstrated the effectiveness of the N-terminal fragment of endostatin in combination with chemotherapy against mammary carcinoma.

Matrix metalloproteinase 2 (MMP2) involves the degradation of the extracellular matrix and the invasion of tumor cells. Endostatin binds to the catalytic domain of MMP2 and blocks endothelial and tumor cell invasion (27). Our docking simulations demonstrated that peptides bind to the catalytic domain of MMP2. Their binding sites do not coincide completely, and the binding energy of ES-SS is lower than ES-Zn. Faye et al. indicated that endostatin binds to Transglutaminase 2 (TG2), an enzyme in the extracellular matrix involves in the angiogenesis process, and arginines 27 and 139 are critical for its binding. The GTP-binding site of TG2 is a potential binding site for endostatin (28). As shown by molecular docking simulation, peptides bind close to the GTP-binding site in TG2 but not coincidentally, and ES-SS interact by more negative binding energy than ES-Zn.

The binding of endostatin to integrin α5β1 on the surface of endothelial cells (ECs) inhibits the migration of ECs (29). Results of molecular docking simulation indicated more negative binding energy of ES-SS compared with ES-Zn. More negative binding energy implicates more binding affinity to the receptors. Briefly, ES-SS form more stable complexes with receptors than ES-Zn, and we can propose that conformational alteration due to the presence of a disulfide bond in the engineered peptide (ES-SS), as determined by MD simulations as well as our previous study, induced superior binding to the receptors and consequently improved its anti-angiogenic and anti-tumor activities. However, more precise analytical and experimental investigations are required to confirm the difference in binding affinities between peptides.

Regulating multiple signaling pathways, less drug resistance and toxic profile in clinical trials makes endostatin a more appropriate drug candidate compared with other anti-angiogenic targeted agents such as monoclonal antibodies (2). However, producing a cost-effective, soluble, stable, and biologically active form of recombinant protein is a significant barrier to the clinical use of endostatin (1). Therefore, considering the

[DOI: 10.22088/IJMCM.BUMS.12.2.120]

potential advantages of peptides, particularly straightforward sensitization, application of peptide fragments like ES-SS instead of recombinant endostatin would be valuable.

In this study, measuring volumes of 4T1 derived mammary carcinoma in mice indicated that ES-SS at a dose of 2.5 mg/kg/day and doxorubicin prohibited tumor growth up to 21% and 35%, respectively, and combination strategy improved considerably antitumor activity of these treatments. No significant weight loss was monitored in mice treated with combined ES-SS + doxorubicin suggesting a favorable toxicity profile of this strategy. We previously observed that ES-SS inhibited the growth of MC4-L2 derived mammary adenocarcinoma up to 30%, 35%, and 46% at doses of 2.5 mg/kg, 0.5 mg/kg, and 50 µg/kg (twice a day) (6). The discrepancy in these two studies could attributed to different tumor types (4T1 vs. MC4-L2) and treatment schedules (daily vs. twice a day). There were no data about the combination of the peptides derived from endostatin and chemotherapeutic drugs. However, a number of researchers have reported the effects of concomitant use of full-length endostatin and cytotoxic drugs like doxorubicin, gemcitabine (30), and paclitaxel (31) in tumor-bearing mice. For example, Xu et al. (2011) indicated that a combination of endostatin (doses of 10, 5, and 2.5 mg/kg/day) and doxorubicin (2.5 mg/kg/4 day) had a significant and synergistic anti-osteosarcoma effect, as well as reducing microvessel density and augmenting apoptotic index, as measured by TUNEL assay, compared to mono-chemotherapeutic regimens (32). Moreover, results reported by Plum et al. (2003) demonstrated that the combination of endostatin (5 mg/kg/day) with doxorubicin (5 mg/kg/4 day) had a synergistic inhibitory effect on the growth of DA-3 mammary tumors in mice (33).

Ki-67 is a key cell proliferation marker and prognostic factor for evaluating outcomes, survival, and the risk of recurrence in patients with breast cancer (34,35). Here, Ki-67 expression in tumors was assessed immunohistochemically, and a significant decrease in Ki-67 index was observed in tumors treated with both ES-SS and doxorubicin. Thus, we proposed that the reduction of Ki-67 is associated with the suppression of tumor growth detected in this study. Une et al. demonstrated that Lenvatinib, an angiogenesis inhibitor, normalized tumor vasculature and reduced hypoxia in the hepatocellular carcinoma in mice. This lead radio-sensitivity enhancement of tumor was treated with both levatinib and radiation. In addition, the number of Ki-67-positive cells was reduced significantly in the combination therapy group compared to the others (36)

Whether the interrelations between endostatin and chemotherapeutic agents are additive or synergistic is questionable. The results of Velde et al. showed additive therapeutic effects of endostatin in combination with doxorubicin in mouse liver metastatic model (37) However, other researchers found that concomitant application of endostatin with doxorubicin had a synergistic effect (32,33,38). Definitely further investigation into the present combination strategy is warranted to answer the debate.

To evaluate the effect of combination therapy on the vascularization of breast tumors, immunohi-stochemical staining of CD31 and CD34 markers were carried out. Accordingly, angiogenesis was inhibited more effectively in tumors treated concurrently with ES-SS and doxorubicin. The anti-vascular effect of doxorubicin has been identified previously through some assays (32,33,38). Our finding corroborates the ideas of Liu et al., who reported that doxorubicin reduced the number of microvessels in tumor sections and affected tumor cells and endothelium directly (38). They proposed that the inhibition of the proliferation of endothelial cells, and down-regulation of VEGF expression are the mechanisms by which doxorubicin

[DOI: 10.22088/IJMCM.BUMS.12.2.120]

improves the anti-angiogenic effects of endostatin. In addition, Itashiki et al. showed that combination of Bevacizumab (5 ml/kg/day), an antiangiogenic drug, with S-1 (6.9 mg/kg/day), a fluoropyrimidine antineoplastic agent, led to the reduction of microvessel density and CD31 positive cells as well as an elevation of apoptotic index in HSC-2 tumor tissues (39).

To elucidate the possible mechanism involved in the anti-cancer activity of our combination therapy, we detected apoptosis by evaluating the expression of Bcl-2 and p53 and the generation of DNA fragmentation in tumor tissues. We found evidence that the combination of ES-SS and doxorubicin induces apoptosis in tumor cells more efficiently than monotherapy, confirming that apoptosis is an important pathway associated with the antitumor activity of these compounds. Prior investigations demonstrated that the expression of Bcl-2 family members, included Bcl-2 and Bclx, were down regulated in MCF-7 and H-196 cancer cell lines treated by doxorubicin (40,41). In addition, activation of p53, and subsequently the induction of apoptosis in tumor cells, is thought to be a key mechanism of action of doxorubicin (42) and its effect on Bcl-2 expression is mediated by p53 pathways (17). Our findings confirm that doxorubicin induces apoptosis in tumor cells, but the related pathways are not clear exactly (17). Induction of apoptosis in endothelial cells and subsequently in tumor cells is one of the mechanisms mediated by endostatin (43,44).

Some studies discovered that cell proliferation prevention and apoptosis induction in tumors are one the mechanism of some combination therapies (36,39). For example, Itashiki et al. indicated that combination of bevacizumab with S-1 chemotherapy suppressed HSC-2 tumor growth in nude mice. Immunohisto-chemically staining of tumor tissues revealed that Ki-67 marker was lower and apoptotic index was higher in mice received combination therapy compared to the monotherapy groups (39). In the present study, we achieved similar results. Our findings further support the idea that angiogenesis prevention and apoptosis induction in tumors are extensively associated. This result also accords with our earlier observations, which showed that a mutated N-terminal fragment of endostatin down-regulates the expression of Bcl-2 in mammary tumors (45). Other signaling pathways should be investigated to achieve more knowledge about the anti-cancer mechanisms of the present study.

In conclusion, the current study demonstrated that concurrent administration of an anti-angiogenic peptide with chemotherapy can lead to superior tumor growth inhibition and apoptosis induction in mouse breast tumor models compared to monotherapy. Docking simulation showed that this peptide interacts with the integrin α5β1, transglutaminase 2, and matrix metalloproteinase 2 with lower binding energy than native peptide. Owing to the advantages of peptides to recombinant proteins or monoclonal antibodies, further preclinical evaluations of this combination treatment appear highly attractive for translation into clinical trials in the future.

Acknowledgment

The authors express their gratitude to the Research Council of the University of Guilan, Rasht, Iran, and Professor Farhad Mashayekhi for his valuable support.

References

1. Mohajeri A, Sanaei S, Kiafar F, et al. The Challenges of Recombinant Endostatin in Clinical Application: Focus on the Different Expression Systems and Molecular Bioengineering. Adv Pharm Bull 2017;7:21-34.

[DOI: 10.22088/IJMCM.BUMS.12.2.120]

2. Li K, Shi M, Qin S. Current Status and Study Progress of Recombinant Human Endostatin in Cancer Treatment. Oncol Ther 2018;6:21-43.

3. Chen J, Yao Q, Huang M, et al. A randomized Phase III trial of neoadjuvant recombinant human endostatin, docetaxel and epirubicin as first-line therapy for patients with breast cancer (CBCRT01). Int J Cancer 2018;142:2130-8.

4. Jie Wang X, Miao K, Luo Y, et al. Randomized controlled trial of endostar combined with cisplatin/ pemetrexed chemotherapy for elderly patients with advanced malignant pleural effusion of lung adenocarcinoma. J BUON 2018;23:92-7.

5. Tjin Tham Sjin RM, Satchi-Fainaro R, Birsner AE, et al. A 27-amino-acid synthetic peptide corresponding to the NH2-terminal zinc-binding domain of endostatin is responsible for its antitumor activity. Cancer Res 2005;65:3656-63.

6. Chamani R, Asghari SM, Alizadeh AM, et al. Engineering of a disulfide loop instead of a Zn binding loop restores the anti-proliferative, anti-angiogenic and anti-tumor activities of the N-terminal fragment of endostatin: Mechanistic and therapeutic insights. Vascul Pharmacol 2015;72:73-82.

7. Kakde D, Jain D, Shrivastava V, et al. Cancer therapeutics-opportunities, challenges and advances in drug delivery. Journal of Applied Pharmaceutical Science 2011:01-10.

8. Frei E, 3rd, Karon M, Levin RH, et al. The effectiveness of combinations of antileukemic agents in inducing and maintaining remission in children with acute leukemia. Blood 1965;26:642-56.

9. Bayat Mokhtari R, Homayouni TS, Baluch N, et al. Combination therapy in combating cancer. Oncotarget 2017;8:38022-43.

10. Liu CJ, Hu T, Shao P, et al. TAS-102 Monotherapy and Combination Therapy with Bevacizumab for Metastatic Colorectal Cancer. Gastroenterol Res Pract 2021;2021:4014601.

11. Chen S, Wei H, Zhao W, et al. PD-1/PD-L1 inhibitors plus anti-angiogenic agents with or without chemotherapy versus PD-1/PD-L1 inhibitors plus chemotherapy as second or later-line treatment for patients with advanced non-small cell lung cancer: A real-world retrospective cohort study. Front Immunol 2022;13:1059995.

12. Yardley DA. Drug resistance and the role of combination chemotherapy in improving patient outcomes. Int J Breast Cancer 2013;2013:137414.

13. An J, Lv W. Endostar (rh-endostatin) versus placebo in combination with vinorelbine plus cisplatin chemotherapy regimen in treatment of advanced non-small cell lung cancer: A meta-analysis. Thorac Cancer 2018;9:606-12.

14. Baluk P, Hashizume H, McDonald DM. Cellular abnormalities of blood vessels as targets in cancer. Curr Opin Genet Dev 2005;15:102-11.

15. Jain RK. Normalizing tumor microenvironment to treat cancer: bench to bedside to biomarkers. J Clin Oncol 2013;31:2205-18.

16. Haibe Y, Kreidieh M, El Hajj H, et al. Resistance Mechanisms to Anti-angiogenic Therapies in Cancer. Front Oncol 2020;10:221.

17. Tacar O, Sriamornsak P, Dass CR. Doxorubicin: an update on anticancer molecular action, toxicity and novel drug delivery systems. J Pharm Pharmacol 2013;65:157-70.

18. Hudis CA. Clinical implications of antiangiogenic therapies. Oncology (Williston Park) 2005;19:26-31.

19. Klement G, Baruchel S, Rak J, et al. Continuous low-dose therapy with vinblastine and VEGF receptor-2 antibody induces sustained tumor regression without overt toxicity. J Clin Invest 2000;105:R15-24.

20. Castelli C, Rivoltini L, Rodolfo M, et al. Modulation of the myeloid compartment of the immune system by angiogenic- and kinase inhibitor-targeted anti-cancer therapies. Cancer Immunol Immunother 2015;64:83-9.

21. Chamani R, Soleimanjahi H, Asghari SM, et al. Re-engineering of the immunosuppressive tumor microenvironment by antiangiogenic therapy. Int J Pept Res Ther 2020;26:539-46.

[DOI: 10.22088/IJMCM.BUMS.12.2.120]

22. Lin Z, Zhang Q, Luo W. Angiogenesis inhibitors as therapeutic agents in cancer: Challenges and future directions. Eur J Pharmacol 2016;793:76-81.

23. Abraham MJ, Murtola T, Schulz R, et al. GROMACS: High performance molecular simulations through multi-level parallelism from laptops to supercomputers. SoftwareX 2015;1:19-25.

24. Chamani R, Taleqani MH, Imanpour A, et al. New insights into short peptides derived from the collagen NC1 alpha1, alpha2, and alpha3 (IV) domains: An experimental and MD simulations study. Biochim Biophys Acta Proteins Proteom 2022;1870:140769.

25. Comeau SR, Gatchell DW, Vajda S, et al. ClusPro: a fully automated algorithm for protein-protein docking. Nucleic Acids Res 2004;32:W96-9.

26. Jelesarov I, Karshikoff A. Defining the role of salt bridges in protein stability. Methods Mol Biol 2009;490:227-60.

27. Lee SJ, Jang JW, Kim YM, et al. Endostatin binds to the catalytic domain of matrix metalloproteinase-2. FEBS Lett 2002;519:147-52.

28. Faye C, Inforzato A, Bignon M, et al. Transglutaminase-2: a new endostatin partner in the extracellular matrix of endothelial cells. Biochem J 2010;427:467-75.

29. Abdollahi A, Hlatky L, Huber PE. Endostatin: the logic of antiangiogenic therapy. Drug Resist Updat 2005;8:59-74.

30. Wu Y, Yang L, Hu B, et al. Synergistic anti-tumor effect of recombinant human endostatin adenovirus combined with gemcitabine. Anticancer Drugs 2005;16:551-7.

31. Li J, Dong X, Xu Z, et al. Endostatin gene therapy enhances the efficacy of paclitaxel to suppress breast cancers and metastases in mice. J Biomed Sci 2008;15:99-109.

32. Xu H, Niu X, Zhang Q, et al. Synergistic antitumor efficacy by combining adriamycin with recombinant human endostatin in an osteosarcoma model. Oncol Lett 2011;2:773-8.

33. Plum SM, Hanson AD, Volker KM, et al. Synergistic activity of recombinant human endostatin in combination with adriamycin: analysis of in vitro activity on endothelial cells and in vivo tumor progression in an orthotopic murine mammary carcinoma model. Clin Cancer Res 2003;9:4619-26.

34. Cabrera-Galeana P, Munoz-Montano W, Lara-Medina F, et al. Ki67 Changes Identify Worse Outcomes in Residual Breast Cancer Tumors After Neoadjuvant Chemotherapy. Oncologist 2018;23:670-8.

35. Fasching PA, Heusinger K, Haeberle L, et al. Ki67, chemotherapy response, and prognosis in breast cancer patients receiving neoadjuvant treatment. BMC Cancer 2011;11:486.

36. Une N, Takano-Kasuya M, Kitamura N, et al. The anti-angiogenic agent lenvatinib induces tumor vessel normalization and enhances radiosensitivity in hepatocellular tumors. Med Oncol 2021;38:60.

37. te Velde EA, Vogten JM, Gebbink MF, et al. Enhanced antitumour efficacy by combining conventional chemotherapy with angiostatin or endostatin in a liver metastasis model. Br J Surg 2002;89:1302-9.

38. Liu F, Tan G, Li J, et al. Gene transfer of endostatin enhances the efficacy of doxorubicin to suppress human hepatocellular carcinomas in mice. Cancer Sci 2007;98:1381-7.

39. Itashiki Y, Harada K, Takenawa T, et al. Antitumor effects of bevacizumab in combination with fluoropyrimidine drugs on human oral squamous cell carcinoma. Oncol Lett 2021;22:730.

40. Sharifi S, Barar J, Hejazi MS, et al. Doxorubicin Changes Bax /Bcl-xL Ratio, Caspase-8 and 9 in Breast Cancer Cells. Adv Pharm Bull 2015;5:351-9.

41. Inoue-Yamauchi A, Jeng PS, Kim K, et al. Targeting the differential addiction to anti-apoptotic BCL-2 family for cancer therapy. Nat Commun 2017;8:16078.

[DOI: 10.22088/IJMCM.BUMS.12.2.120]

42. Wang S, Konorev EA, Kotamraju S, et al. Doxorubicin induces apoptosis in normal and tumor cells via distinctly different mechanisms. intermediacy of H(2)O(2)- and p53-dependent pathways. J Biol Chem 2004;279:25535-43.

43. Ling Y, Lu N, Gao Y, et al. Endostar induces apoptotic effects in HUVECs through activation of caspase-3 and decrease of Bcl-2. Anticancer Res 2009;29:411-7.

44. Folkman J. Angiogenesis and apoptosis. Semin Cancer Biol 2003;13:159-67.

45. Chamani R, Asghari SM, Alizadeh AM, et al. The antiangiogenic and antitumor activities of the N-terminal fragment of endostatin augmented by Ile/Arg substitution: The overall structure implicated the biological activity. Biochim Biophys Acta 2016;1864:1765-74.

[DOI: 10.22088/IJMCM.BUMS.12.2.120]